Original Article

Unlocking the Power of GO in Next-Gen Concrete: Strength, Hydration, and Microstructural Evolution

P. M. Walunjkar¹, M. N. Bajad²

^{1,2}Sinhgad College of Engineering, Savitribai Phule Pune University, Pune, Maharashtra, India.

¹Corresponding Author: pwalunjkar035@gmail.com

Received: 07 September 2025 Revised: 08 October 2025 Accepted: 06 November 2025 Published: 29 November 2025

Abstract - This study explores the impact of incorporating 0.03% Graphene Oxide (GO) into cement paste and concrete, with a focus on mechanical properties, microstructure, and hydration product evolution over 1 hour to 120 days. Key mechanical parameters—compressive, split tensile, and flexural strength—were evaluated at 3, 7, and 28 days. Results show significant improvements: flexural strength increased by 38-48%, split tensile strength by 22-35%, and compressive strength by 21-32%. GO accelerates hydration, promoting early formation of needle-like and flower-like crystals, enhancing development of Calcium Silicate Hydrate (C-S-H) gel, ettringite, and portlandite. SEM, XRD, and EDAX analyses revealed early rod-like crystals, which disappear with matrix densification but reemerge by day 7 and transform into flower-like forms by day 28. At 60 days, polyhedral and flower-like crystals surround residual needle-like structures, leading to a dense matrix by day 120 with icosahedral and cubic CaCO₃ crystals. XRD confirmed the presence of fullerite C₆₀, suggesting GO moderates early cement setting. Transient phases, such as magnesite and eitelite, emerge from magnesium-related reactions, improving the density and refining pores. A 90% increase in Ca (OH)₂ at day 7 transforms into CaCO₃, resulting in an average of 82% of the final 28-day mechanical strength within 7 days, which is 26% higher than that of conventional concrete. EDAX confirms GO's oxygen stabilization and consistent concentration over time. CH crystal size increased from 64 nm to 82 nm by day 7 and then stabilized, indicating improved crystallization. Portlandite and ettringite both exhibit hexagonal structures with lattice parameters a = 3.59 Å, c =4.90 Å, and a = 11.23 Å, c = 21.44 Å, respectively. An average Ca/Si ratio of 2.06 suggests improved tensile strength and stiffness. These results underscore the potential of GO as an innovative additive for developing high-performance concrete, contributing to the advancement of modern sustainable construction.

Keywords - C-S-H bonding, Ca/Si ratio, EDAX analysis, Graphene Oxide (GO), Interfacial Transition Zone (ITZ), SEM, XRD.

1. Introduction

Concrete, an essential and versatile material, plays a pivotal role in modern construction, powering everything from skyscrapers to bridges. At its core is ordinary Portland cement, prized for its affordability, water resistance, and exceptional compressive strength. Nonetheless, despite these benefits, concrete is vulnerable to cracking under stress, and its often inadequate tensile and flexural strengths can lead to premature failure. To overcome these limitations, steel reinforcement has long been the go-to solution [1]. However, Portland cement is also a major environmental culprit, contributing to over 80% of the emissions of greenhouse gases linked to the manufacture of concrete. This raises serious concerns, prompting the UNFCCC to pledge a reduction in CO₂ emissions by 2030 as part of the global climate action plan [2]. Meanwhile, exciting innovations in materials science are paving the way for stronger, more sustainable concrete. Nanotechnology opened new frontiers, mixtures groundbreaking incorporating nanoparticles showing remarkable potential to improve performance [3]. Among the most promising advances is graphene —a material that has taken the world by storm due to its extraordinary properties. Concrete enhanced with graphene boasts a mindboggling tensile strength of over 1.3 TPa and an Elastic modulus (E) of 425 GPa, making it not only stronger but also more durable. Beyond its mechanical benefits, graphene is a game-changer for sustainability, helping to reduce concrete's carbon footprint and pushing the industry closer to achieving greener, more eco-friendly building practices [4]. With its unparalleled characteristics, graphene is rapidly emerging as a transformative force that could redefine the future of construction. Graphene Oxide (GO), a form of graphite that has undergone modification by attaching graphene layers and various oxygen-containing functional groups, also shows outstanding promise. While it maintains structural similarities to graphene, because of these oxygen attributes, GO has special characteristics [5]. There is a significant gap in the literature regarding the effects of incorporating 0.03% GO into cement paste on its mechanical strength and microstructural characteristics, including paste texture, pore distribution,

hydration products, and crystalline phase development. Few studies have comprehensively investigated these aspects using Scanning Electron Microscopy (SEM), X-Ray Diffraction (XRD) analysis, and Energy Dispersive X-ray Analysis (EDAX) across some curing intervals. This paper aims to investigate how GO affects mechanical strength parameters like compressive, split tensile, and flexural strength, along with microstructural parameters such as the paste's texture, pore distribution, and the development of different hydration components, such as needle-shaped crystals and designs resembling flowers. It examines how GO influences key hydration products, including Calcium Silicate Hydrate (C-S-H) gel, ettringite, and portlandite. The study also investigates how GO modifies the pore size, distribution, and morphology of cement paste, using SEM analysis.

Additionally, it presents chemical composition analysis of the phases within the paste, identifies elemental distributions, and detects trace components using EDAX analysis. Furthermore, the paper identifies various crystalline phases such as C–S–H gel, Portlandite, ettringite, monosulphate, and calcium carbonate through XRD analysis. It tracks phase evolution over time and examines carbonate formation at intervals of 1 hour, 7 hours, 24 hours, 7 days, 28 days, 60 days, and 120 days.

2. Review of the Relevant Literature

The literature review on mechanical strength (such as compressive strength, split tensile strength, and flexural strength) and microstructural characteristics (such as paste texture, pore distribution, and the formation of various hydration components) is covered in the discussion as follows.

Devasena and Karthikeyan conducted [6] experimentation on M25 GO mixed concrete with 0%, 0.05%, 0.1%, and 0.2% dosages and obtained a rise of 9.95% in the case of compressive strength, 0.95% for split tensile strength, and 2.34% for flexural strength. Antonio et al. [7] studied the effect of the addition of GO at 2%, 4%, and 6% in the case of M35 concrete. The maximum compressive strength was improved by 57% at 2% GO and flexural strength by 65% at 4% GO. Shareef et al. [8] worked on low dosages of 1% and 2% GO with M25 grade concrete. The maximum rise of 7% at 1% GO and 17% at 2% GO was found in the case of compressive strength. The highest elevation in split tensile strength was obtained as 17.41% for 1% and 28% for 2% of GO. Srikanth and Ashok [9] worked on M30 and M40 concrete with 0%, 5%, 10%, 15%, 20%, and 25% GO, along with superplasticizers. The rise of 4.29% and 2.49% for compressive, 13.54% and 10.26% for split tensile, and 11.03% and 7.43% for flexural strength was obtained, respectively. Jinwoo et al. [10] worked with a nominal concrete mix (1:2.11:2.63) in which GO flakes were added by the cement weights of 0.01%, 0.05%, 0.5%, and 1% in dry and wet stages. In both stages, compressive strength was increased by 19.6% and 25.5% respectively, while a rise in flexural strength was obtained as 28% and 37.3% respectively, at 0.05% GO. Chen et al. [11] conducted experimentation on mix proportion (1:1.95:2.93) with 0.02% and 0.08% GO, along with 19% and 7.5% by coal ash and silica fume of cement weight. It gave a 12.65% rise in compressive strength at 0.08% GO. Du et al. [12] achieved the rise of compressive strength by 55.8% at 0.1% GO for (OPC) mixed concrete with a 1:1.5:1.5 ratio. Akarsh et al. [13] worked on M50 concrete with GO of 0.05%, 0.1%, 0.15%, and 0.2% by quantity of cement with 3%, 5%, 7%, and 10% of silica fume. The ultimate rise of 29.5% was obtained at 0.15% GO and 7% silica fume. The experimentation of OPC mixed concrete (1:1.86:2.89) with 0.02%, 0.04%, 0.06%, and 0.08% GO was done by Devi and Khan [14], which gave rise to 22% for both compressive and split tensile strength at 0.08% GO. Xu and Fan [15] worked on OPC mixed concrete (1:1.86:2.57) with 0.01%, 0.03%, and 0.05% GO. It gave rise to 34.8% in compressive strength with 0.03% GO at 200 salt-freezing iterations. Chen et al. [16] worked on M40 concrete mix proportion (1:1.56:2.97) with 0.02%, 0.05%, and 0.08% GO. The highest rise in compressive strength and flexural strength was obtained as 12.65% and 7.3% at 0.08% GO. Chavan and Karriappa [17] worked on M30 concrete with 0%, 0.25%, 0.50%, and 0.75% GO, which gave the rise of 7.5% and 8.9% in compressive strength and split tensile strength at 0.75% GO. Zaid et al. [18] did a study on a 1:1.85:2.87 concrete proportion with 0.03%, 0.06%, 0.09%, and 0.12% GO with steel fibers. It gave a rise to 26% and 21% for compressive strength and split tensile strength at 0.12% GO. Jahami et al. [19] 1:1.65:3.42 mix proportion concrete with 0.02%, 0.035%, and 0.05% GO. It found the rise of 19.2% and 18.5% for compressive strength and split tensile strength at 0.05% GO. Kaushik et al. [20] worked on concrete mixes of grades 15, 20, 25, 30, 35, and 40, respectively, with 0.12%, 0.14%, and 0.16%, and 0.20%, along with gypsum. The ultimate rise of 15% was achieved at 0.16% GO in the case of compressive strength and split tensile strength.

Adding GO to substances made from cement changes their microstructure, which is crucial for improving their macroscopic performance, according to a number of studies. Two crucial elements of the microstructural characteristics of cement-based materials are the microstructure of the Interfacial Transition Zone (ITZ) and the microstructure of hydration products. Murali et al. [1] discovered through microstructural tests that adding only 0.03-0.05% GO to the composite enhances hydration, forming an interconnected structure that links pores, boosts compactness, and significantly improves mechanical performance. Lv et al. [2] presented SEM images of cement paste reinforced with varying concentrations of GO. When GO is not present, the hydration products are mostly made up of haphazardly stacked needle- and rod-shaped crystals. Flower-like crystals start to form once 0.01-0.03 weight percent GO is added, and they gradually get denser as the hydration products mix. The hydration products change into regular, well-defined

polyhedral crystals with 0.04–0.05 weight percent GO, greatly increasing the structure's density and compactness. According to Lv et al., in samples with very little GO content (0.01-0.04 wt.%), the hydration products become increasingly denser as the cure age increases. The structure becomes increasingly compact and refined as the rod-like crystals almost vanish. After 7 days, there was a rise in compressive strength, and following a 28-day cure period, massive polyhedral crystals formed. High porosity, low strength, and a buildup of Ca (OH)2 are typical characteristics of this zone, which makes it extremely vulnerable to crack formation and spread [3]. When GO is added, chemical reactions are accelerated, hydration products develop and crystallize more quickly, and the material changes into a stronger, more resilient structure [4]. According to Lee and Park [5], the ITZ has a significant influence on the permeability and strength of cement hybrids. The surface and borders of pure mortar are rough, extremely porous, and rife with flaws, which compromise structural integrity, according to Yan et al. [21]. The cement matrix became smooth and firmly compacted with the addition of 0.02 weight percent GO, creating a more homogeneous structure, although the ITZ remained a vulnerable weak point. However, with a GO content of up to 0.04 wt%, the density of the ITZ increased dramatically, resulting in a much stronger and more cohesive structure. Long et al. [22] studied recycled fine aggregate cement mortar and observed that after 7 days, the control sample (without GO) exhibited a boundary layer with high porosity, weak bonding, and a limited quantity of hydration products. In contrast, samples with GO showed reduced porosity, improved bonding, and a greater quantity of hydration products.

For their research, all of the writers in the literature study employed GO content between 0.01 and 0.04 weight percent. The optimal dose for increasing the microstructure of GOmodified cement paste and its compressive, flexural, and split tensile strengths was determined by Murali et al. [1] to be 0.03%. The development of thick hydration products and flower-like crystals was noted by Lv et al. [2], which amplified the toughness effect. Lv et al. observed a similar observation [3]. Liulei Lu and Dong Ouyang [23] reported the emergence of fibrous crystals within pores and improvements in flexural strength. GO was also found to promote the transformation of large micropores into smaller ones, refining pore size and distribution, as observed by Udumulla et al. [24]. Bridging among hydration products was noted by Wang et al. [25]. Xu and Fan [15] recorded a maximum increase of 34.83% at a GO dosage of 0.03% in compressive strength. Using 0.03% ballmilled GO, Jing G.J. et al. [26] showed a 28% rise in the heat of hydration and a 9% enhancement in compressive strength. Qureshi et al. [27] showed a 79% increase in cement mortar's tensile strength, whilst Kang et al. [28] and Zhao et al. [29] reported increases of 40% and 25%, respectively.

This study focuses on GO dosages of 0.00%, 0.03%, 0.05%, 0.60%, 1.00%, and 2.00%, which strike a balance

between performance and cost-efficiency. Dosages exceeding 2% were found to offer little improvement in the concrete's strength, rheological properties, and density, resulting in diminishing returns. Additionally, such high dosages are economically unfeasible for practical use.

2.1. Research Discrepancies

The literature on the precise effects of adding 0.03% GO to cement paste is noticeably lacking. The literature reveals a notable gap concerning the specific effects of incorporating 0.03% GO into cement paste. Particularly with respect to mechanical strength and microstructural parameters such as paste texture, pore distribution, hydration products, and crystalline phase development.

Limited research has comprehensively examined the effects of GO on key hydration products, pore size and morphology, crystal formation, and phase transitions over time. Moreover, there is a lack of studies that analyze these parameters using SEM, XRD, and EDAX in a unified framework across multiple curing intervals—specifically at 1 hour, 7 hours, 24 hours, 7 days, 28 days, 60 days, and 120 days.

2.2. Scientific Relevance and Novelty of the Present Study

Nowadays, graphene derivatives are being incorporated into cement concrete more than ever, unlocking a new level of performance by significantly enhancing its microstructural properties. Among these, GO stands out as a more cost-effective alternative to produce both single-walled and multiwalled carbon nanotubes, which makes it a desirable choice for a variety of uses [30].

- This study explores several key research implications of incorporating GO into cement paste.
- Examining cement paste combined with GO at an extremely small quantity of 0.03%.
- Analysis of microstructural parameters such as paste texture, pore distribution, various hydration products, flower-like patterns, and crystals exhibiting a needleshaped structure.
- Evaluation of GO's effect on key hydration products, such as C–S–H gel, ettringite, and portlandite.
- Examination of GO's influence on the cement paste's pore size and distribution.
- Chemical composition analysis of phases within the paste, including identification of elemental distributions and detection of trace components.
- Assessment of GO's influence on crystalline phases such as C-S-H gel, portlandite, ettringite, monosulphate, and calcium carbonate—covering aspects such as diffraction peaks, phase evolution over time, and carbonation.
- Study of the effect of GO on crystal size and growth duration.
- Assessment of how GO incorporation affects the calciumto-silicon (Ca/Si) ratio over time.

- Influence of GO on mechanical strength.
- Monitoring of transition phases in GO-mixed cement paste at multiple curing intervals (1 hour, 7 hours, 24 hours, 7 days, 28 days, 60 days, and 120 days), using SEM, XRD, and EDAX analyses.

Based on these findings, GO can be effectively applied in real-world construction practices and on-site applications.

2.3. Mechanical Strength Determination

Six different M35-grade concrete mixes were prepared, with three specimens cast for each mix and test, following the guidelines of IS 456:2021 and IS 10262:2019. The water-tocement ratio for all mixes was maintained at 0.4 by weight of cement. GO powder was added to the mixes M0, M1, M2, M3, M4, and M5 in proportions of 0.00%, 0.03%, 0.05%, 0.60%, 1.00%, and 2.00%, respectively. To ensure efficient dispersion, GO was combined with Dr. Fixit 101LW PC solution along with the required amount of mixing water. The effect of this plasticizer was accounted for by adjusting the water-cement ratio during the mix design calculations. The consistency of the concrete mixes was verified at specific intervals using the slump test. The mix composition was maintained at 400:796:1145 kg/m³ (cement: fine aggregate: coarse aggregate), corresponding to a ratio of 1:1.9:2.8. Both air-dried coarse and fine aggregates were used for the mix. First, cement and fine aggregate were incorporated for two minutes in a mechanical mixer that complied with IS 1791:2020 and IS 12119:2018. Following that, coarse aggregate was added and mixed for two minutes and thirty seconds at a moderate pace. Water was added to the mixer using water-measuring instruments, and a hand mixer was used to mechanically whisk the water for one and a half minutes. The functionalized GO water-dispersed solution was then added, and for an additional 1.5 minutes, it was swirled at a moderate pace. After adding the pre-mixed solution to the dry-mixed cement and aggregates, the mixture was moderately agitated for two and a half minutes. Until the components were evenly distributed and the mass had a consistent color and texture, the mixing process was continued.

The curing of concrete samples was carried out as per IS 456:2021. The samples were watered for an adequate duration at 27°C in the concrete technology lab curing tank, where they were immersed for the desired period. The water's pH was preserved in an array of 6 to 8. A time lag of less than 1 hour was maintained between the extraction of samples from the curing tank and testing.

According to IS 456:2021 and IS 10086:2021, 150 mm x 150 mm x 150 mm cubed concrete was used to evaluate compressive strength. The specimens aged 28 days were tested using a Compression Testing Machine (CTM) with a capacity of 2000 kN, in accordance with IS 516:2022. The split tensile strength test was computed in accordance with the requirements of IS 5816:2021. The cylindrical specimens,

measuring 150 mm in diameter and 300 mm in height, were prepared following IS 456:2021 and IS 10086:2021. A force with an intensity ranging from 1.2 to 2.4 N/ (mm²/min) was applied and gradually increased without causing any shock. The load increased at an average rate of 140 kg/cm²/min without shock until the ultimate load was reached. After proper mixing, curing, and drying, the specimens were evaluated at 3, 7, and 28 days.

3. Microscopic Structure Analysis

3.1. Sample Preparation of GO with Cement

GO was added at an optimal dosage of 0.03% by weight of cement (based on mechanical strength results) into distilled water to produce a suspension of nanoparticles. The ultrasonication process was performed using an ultrasonic meter to effectively disperse the GO in the aqueous solution. As shown in Figure 1, the process was conducted at 400 W for 15 minutes. To prevent overheating, the water temperature was kept at 30°C. After sonication, the GO was thoroughly mixed with distilled water, forming a thick black solution. Cement was then added to this solution and stirred continuously, gradually increasing the speed from slow to fast over a 2-minute interval using a wired whisk. To distribute the GO in the water-based solution, the sample was subjected to ultrasonication using an ultrasonic meter. The process was carried out, as shown in Figure 1, at 400 W for 15 minutes, with the water temperature maintained at 30°C to prevent overheating. After the ultrasonication process, the GO powder was thoroughly mixed with distilled water, forming a thick black solution. After that, cement was incorporated into this solution and stirred continuously, gradually increasing the mixing speed from slow to fast over a 2-minute interval using a wire whisk.

An FEI Nova NanoSEM 450, which has exceptionally low-vacuum capabilities and ultra-high-resolution lowvoltage imaging, was used to conduct Field Emission Scanning Electron Microscopy (FESEM). The device provides a resolution of 1.8 nm at 3 kV and 30 Pa, 1.0 nm at 15 kV, and 1.4 nm at 1 kV. It has detectors for lens, Secondary Electrons (SE), Backscattered Electrons (BSE), and Through-Lens Detectors (TLD). A Bruker XFlash 6I30 detector, which is renowned for its exceptional energy resolution (123 eV at Mn Kα and 45 eV at C Kα) and element detection range from beryllium (Be, atomic number 4) to americium (Am, atomic number 95), was used to perform Energy-Dispersive X-Ray Spectroscopy (EDXS). For SEM observation, each specimen, weighing approximately 1 g, was attached to a conductive film on the specimen stage. To ensure the sample remained securely in place, high-pressure gas was sprayed onto it. Since the solidified paste had weak conductivity, gold was applied to the powder samples before testing. XRD was performed using a Bruker D8 Venture equipped with a Cu Ka microfocus source, and the analysis was supported by Bruker Smart Apex software. The device has an XYZ goniometer head and a Kappa (4-circle) goniometer. It has an active area of 10 cm

 \times 10 cm and is equipped with an air-cooled Photon 100 CMOS detector. A Kryoflex II and an Oxford Cryostream 700 Plus low-temperature device are also included in the system, allowing for a temperature range of less than 90 K to 400 K. Copper (Cu) was used as the target material in the XRD examination. In order to identify and measure the composition of the nanoparticles, the peak positions and intensities of the samples were compared with reference patterns from several diffraction databases [31]. To prevent any moisture interference and ensure accurate results, the samples were kept dry and maintained in a vacuum atmosphere prior to testing. After aging for a predetermined time, the samples were submerged in anhydrous ethanol to halt the hydration process. The samples were then soaked, filtered, and dried in an oven at 35°C for 12 hours. Once dried, the samples were collected and stored in a standard conditioning chamber before being subjected to SEM and XRD analyses at 7 and 28 days, respectively [32]. SEM and XRD analyses were performed on the produced samples at different curing intervals (1 hour, 7 hours, 24 hours, 7 days, 28 days, 60 days, and 120 days) after they were placed in a standard conditioning chamber.

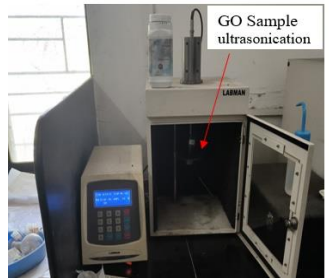




Fig. 1 Sample prepared with GO and distilled water using an ultrasonicator

4. Results and Discussion

4.1. Mechanical Strength Assessment

The compressive strength was obtained with various dosages of GO, as shown in Table 1. M1 mix, in contrast with the non-GO group, shows the highest increase of 32% after 3 days, 27% after 7 days, and 21% after 28 days. For a similar portion of concrete, Zaid et al. [18] saw a 26% rise at 0.12% GO, whereas Jahami et al. [19] saw a 19% increase at 0.05% GO. Devi and Khan [33] also observed a 33% increase with recycled coarse aggregate and 0.1% ball-milled GO and a 22% increase with 0.1% GO and recycled aggregate.

Table 1. Compressive strength of GO additive concrete

Sr. No	Mix	Average compressive strength (N/mm²)		
		3 days	7 days	28 days
1	M0	14.52	21.63	43.40
2	M1	19.21	27.64	52.88
3	M2	18.87	20.93	45.30
4	M3	18.85	20.90	44.93
5	M4	18.82	20.71	44.32
6	M5	18.59	20.40	42.95

The split tensile strength was obtained with various dosages of GO, as shown in Table 2. M1 mix, in contrast with the non-GO group, shows the highest increase of 35% after 3 days, 25% after 7 days, and 22% after 28 days. In the case of cement, fly ash, and silica fume mixed concrete with GO at 0.025%, 0.05%, and 0.075%, Chu et al. [34] saw a similar effect. At a maximum of 0.05%, the splitting tensile strength rose by 29.54%.

Table 2. Split tensile strength of GO additive concrete

Sr. No	Mix	Average split tensile strength (N/mm²)		
		3 days	7 days	28 days
1	M0	2.12	3.04	4.67
2	M1	2.88	3.81	5.73
3	M2	2.75	3.67	5.44
4	M3	2.74	3.60	5.40
5	M4	2.33	3.42	5.12
6	M5	2.09	2.97	4.69

The results of flexural strength obtained with various dosages of GO, as shown in Table 3, M1 mix, in contrast with the non-GO group, show the highest increase of 48% after 3 days, 47% after 7 days, and 38% after 28 days. For M25 grade concrete, Devasena and Karthikeyan [6] obtained an increase of 2.34% at 0.1% GO. For M35 grade concrete, Antonio et al. [7] discovered a 65.2% increase at 4% GO. For the nominal mix (1:2.11:2.63), Jinwoo et al. [10] found that the wet mixing of 0.05% GO increased by 37.3% and the dry mixing increased by 28%. An increase of 7.38% for M40 concrete at 0.08% GO was reported by Chen et al. [16].

Table 3. Flexural strength of GO additive concrete

Sr. No	Mix	Average flexural strength (N/mm²)		
		3 days	7 days	28 days
1	M0	2.75	3.74	5.76
2	M1	4.08	5.52	8.0
3	M2	3.85	4.56	7.2
4	M3	3.80	4.45	7.08
5	M4	3.02	4.40	6.91
6	M5	2.9	4.00	5.85

4.2. Analysis of SEM Images of GO Mixed Cement Paste After 1hr,7hr,24hr,7 Days,28 Days, 56 Days, and 120 Days

The SEM images after 1 hour of hydration of the GO-mixed cement paste are shown in Figure 2. Part (a) shows bundles of fibrous structures, sheaves, plumose formations, and fine granular structures of calcium silicate. Ettringite growth is observed from the hydration layers shown in Part (b). Area shots 1 and 2 from Part (c) demonstrate that the hydration products contain a significant amount of oxygen and carbon, which also include silicon and calcium, as verified by EDAX results. This suggests that either crystalline or amorphous C-S-H, such as Jennite, is present and is what gives

the cement paste its strength. Similar observations were reported by Jinwoo An and Matthew McInnis [10]. Part (d) shows a close-up view of ettringite. SEM Figure 3 shows the morphology of the GO-mixed cement paste after 7 hours of hydration. Part (a) displays large agglomerated particles forming extensive clusters, a characteristic also observed by Lu et al. [23], which was identified as poorly compacted and lumpy hydration products.

Significant growth of needle-like ettringite structures is visible on the cement paste's surface in Parts (b) and (d), particularly around pore regions. These needle-shaped hydration crystals form a strong, interconnected network within the matrix, significantly enhancing compressive strength, as identified by Subramani and Ganesan [35] and Shaoqiang Meng et al. [32].

Point shots 3 and 4 in Part (c) represent ettringite, a byproduct of cement hydration, which does not contain carbon. This suggests that the GO, which shows approximately 60% carbon content in EDAX analysis, may support C-S-H with its elevated modulus and tensile strength, or it may serve as a nucleation site for C-S-H creation. This type of morphology resembles cement hydration crystals, also reported by Jinwoo An and Matthew McInnis [10].

SEM Figure 4 shows the morphology of the GO-mixed cement paste after 24 hours of hydration. The rise in the C-S-H layer and barrier quality of GO contributes to the densification of hydration products, ultimately resulting in pore reduction, as observed in Parts (a) to (d). The densification of hydration products initiates at this stage.

This observation was consistent with studies conducted by Liulei Lu and Dong Ouyang [23] and Wengui Li et al. [36]. Additionally, the Figure shows that the GO sheets and the surrounding cement matrix have a tight bond, with an anchoring effect observed—particularly relevant for ultrahigh-strength concrete.

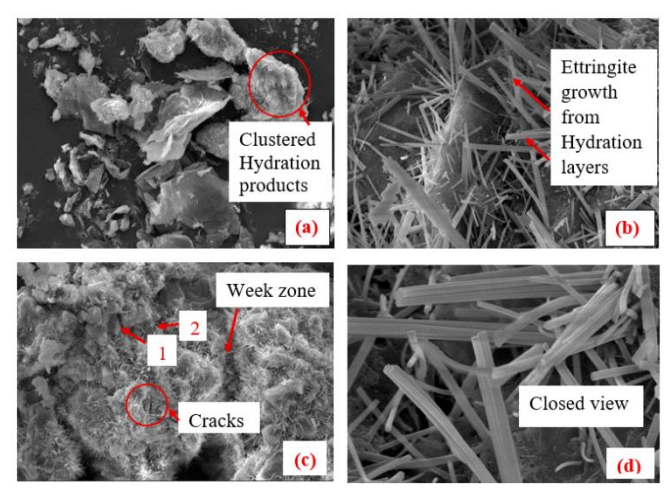


Fig. 2 SEM images of GO mixed cement paste after 1 hour

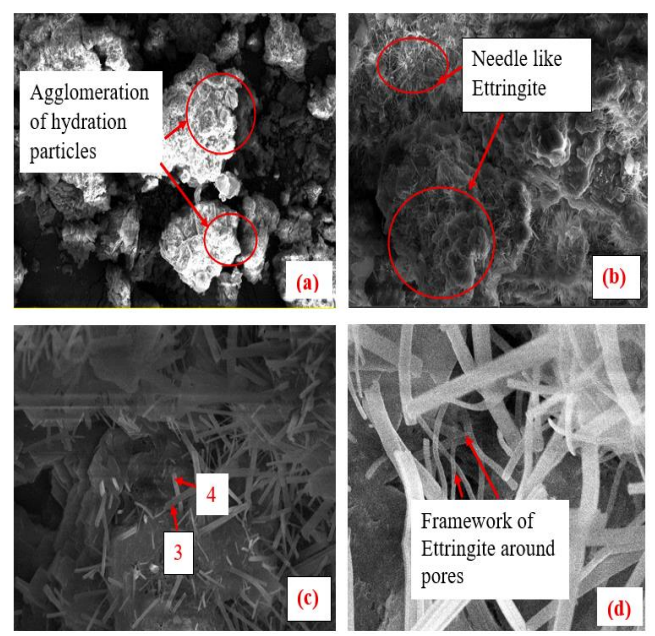


Fig. 3 SEM images of GO mixed cement paste after 7 hr

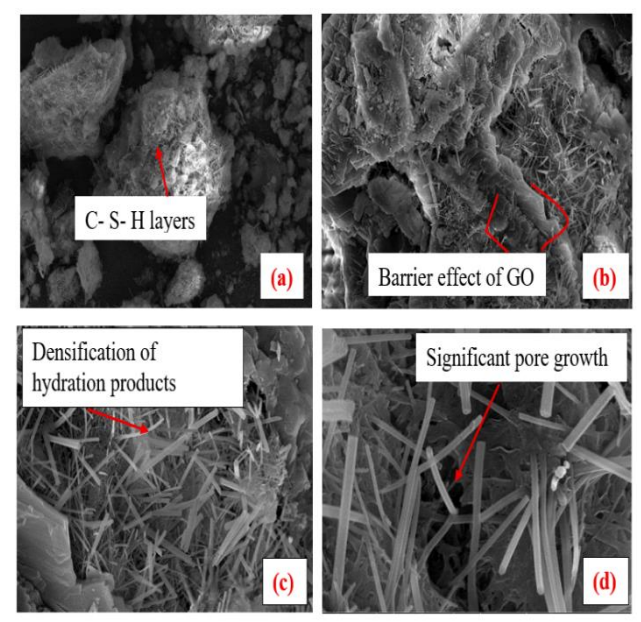


Fig. 4 SEM images of GO mixed cement paste after 24 hr

In the hydration growth phase, the functional reactive groups on GO, such as -OH, -COOH, and -SO₃H, interact with C₂S, C₃S, and C₃A, during which the reaction is temporarily retarded, as reported by Al-Dhawai et al. [37]. As hydration progresses and the products become denser, the rod-like crystals begin to disappear.

Following the retarding phase, new rod-shaped crystals begin to grow on the GO surface and develop into flower-like structures, as illustrated in SEM Figure 5 (a)–(d). A similar morphological pattern was reported by Shenghua Lv et al. [2] after 7 days of hydration.

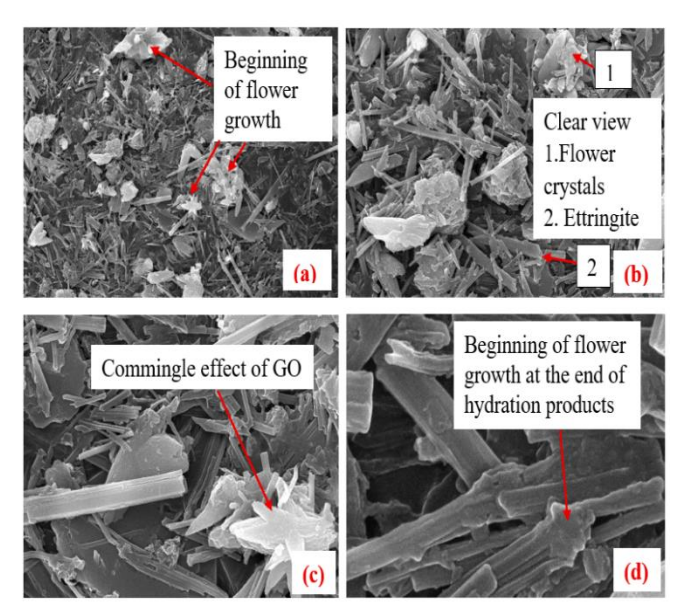


Fig. 5 SEM images of GO mixed cement paste after 7 days

As hydration continues, the products become denser, and the rod-like crystals completely disappear after 28 days. New rod-shaped crystals start to form and develop into structures that resemble flowers, as shown in Figure 6 (a)–(d).

A weak point in cement-based materials, the zone of interfacial transition, or ITZ, between cement paste particles is characterized by poor strength, large porosity, and Ca (OH)₂ concentration, making it susceptible to crack initiation and propagation. A similar surface morphology was reported by Changjiang Liu et al. [38]. This results in the formation of a more compact and less porous surface, which tends to increase durability and high mechanical properties.

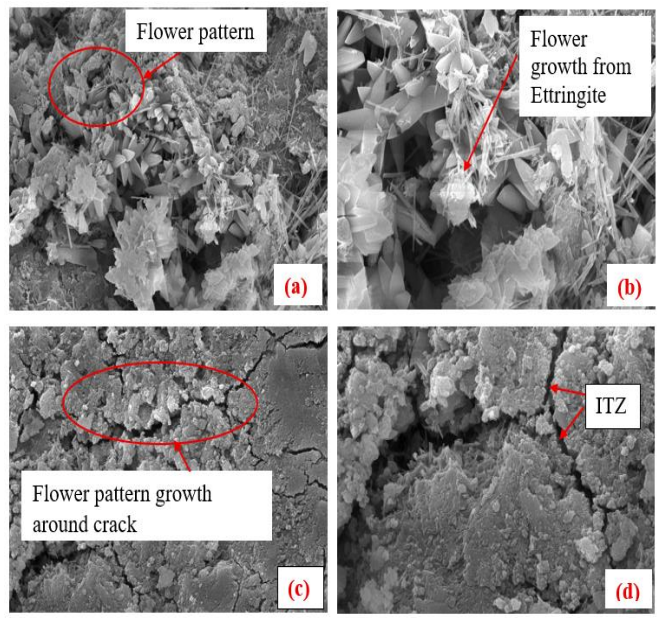


Fig. 6 SEM images of GO mixed cement paste after 28 days

The formation of a network within the pores helps to fill microcracks, as shown in Figure 7(a). A combination of flower-like and polyhedral crystals was observed around the needle-like structures, as seen in Figure 7(d). After 60 days, the crack lines disappeared, and AFM images confirmed surface refinement, as shown in Figure 7(c); a dense, hardened paste surface with an icosahedral shape was observed. The flower-like crystals had mostly disappeared from the surface, as shown in Figure 8(a) after 120 days. The transition of calcium carbonate was observed in three phases: i) Formation of a single CaCO₃ cubic crystal with rhombohedral morphology, ii) A transient phase of CaCO₃ near the growing crystal, and iii) Formation of a second CaCO₃ crystal phase, as shown in Figure 8(b).

4.3. SEM Analysis of 0.03% GO Mixed Cement Paste – Transition Phases

The transition phases of GO-mixed cement paste at various time frames (1 hour, 7 hours, 24 hours, 7 days, 28 days, 60 days, and 120 days) are shown in SEM Figure 9. The Figure primarily illustrates the following transition phases: heat of hydration, formation of ettringite, the barrier effect of GO, growth of flower-like patterns, densification due to GO, the looping effect within pores, and the densification of the hardened paste with the formation of an icosahedral shape.

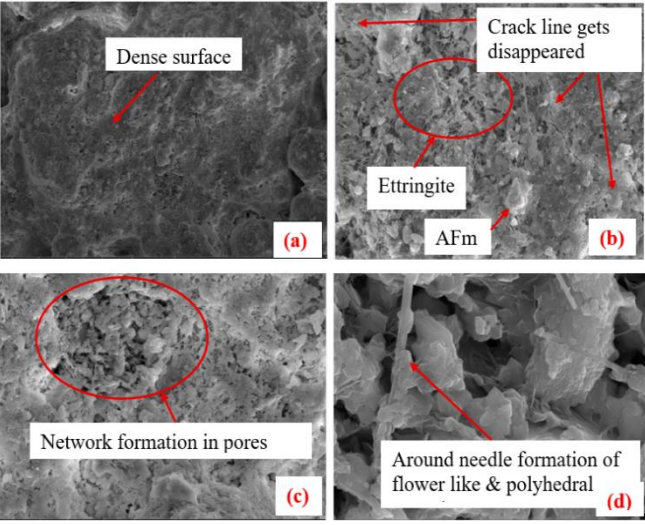


Fig. 7 SEM images of GO mixed cement paste after 60 days

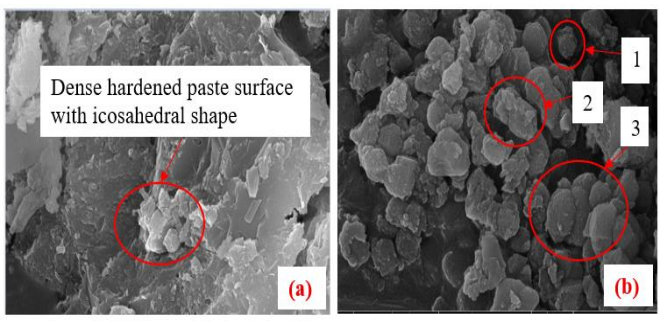


Fig. 8 SEM images of GO mixed cement paste after 120 days

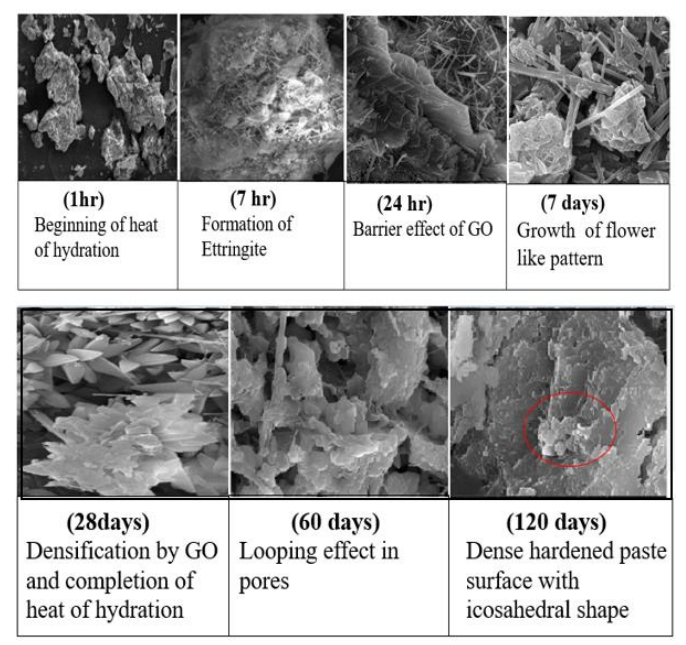


Fig. 9 SEM images of GO mixed cement paste - Transition phases

4.4. XRD Analysis of 0.03% GO Mixed Cement Paste - Transition Phases

An XRD is a powerful tool widely used by researchers to investigate the intricate crystalline structure of materials, providing information about atomic arrangement and properties (Hu et al., [39], Long et al., [22], Liu et al., [40], Chintalapudi & Pannem, 2020 [41], Kaur & Kothiyal [42], Li et al., [43], and Qureshi & Panesar [44]). The peaks of calcite (CaCO₃), eitelite (Na₂Mg (CO₃) ₂), and lead oxide carbonate (Pb₃CO₅) were observed in this phase. The formation of ettringite and dolomite was also observed during the process. Fullerite (C₆₀), a closed mesh form of graphite, was found in a quantity of 49%, representing GO. It was already present in the early-stage liquid cement, which is useful for controlling the mixture sets.

According to Jinwoo An and Matthew McInnis [10], fullerite is a colorless to yellow mineral crystallizing in the trigonal system, as shown in Figure 10. Magnesite and eitelite are the main characterized transient phases during magnesium formation after 1 hour. The large quantities of calcium silicate (82%) and calcite (43%) indicate incomplete hydration at this stage, suggesting that a significant number of cement clinkers remained unreacted (P.K. Akarsh et al., [45]) after 7 hours. A significant amount of hydration items, including calcium hydroxide (Ca (OH)₂) (82%) and calcium silicate (84%), are visible in this phase after 24 hours, indicating early heat of hydration promotion by GO. As the GO concentration increases, the levels of CH and C-S-H surge, highlighting GO's role as a powerful nucleation site that initiates C₃S hydration, having an enormous effect on cement hydration during the growth and nucleation stages, as identified by Lu et al. [23], Cui et al. [46], and An et al. [47]. The rise in SiO₂ from the previous stage, i.e., from 6.9% to 8.59%, and from 8.59% to 11.84%, indicates the progress of the heat of hydration, as shown in Figure 10 [45]. The 7-day results indicate a rise in Ca (OH)₂, with a significant increase of 90%, indicating the product of heat hydration in large quantities. Calcium Hydroxide is changed into calcium silicates by silica fumes, and the calcium silicates that result use GO as nucleation sites. As illustrated in Figure 10, the rise in Ca (OH)₂ suggests an improved hydration process brought on by the existence of silica fumes. Thus, GO concrete demonstrates higher strength than normal conventional concrete in the early stages. Shenghua Lv et al. [2] also observed similar findings in their studies.

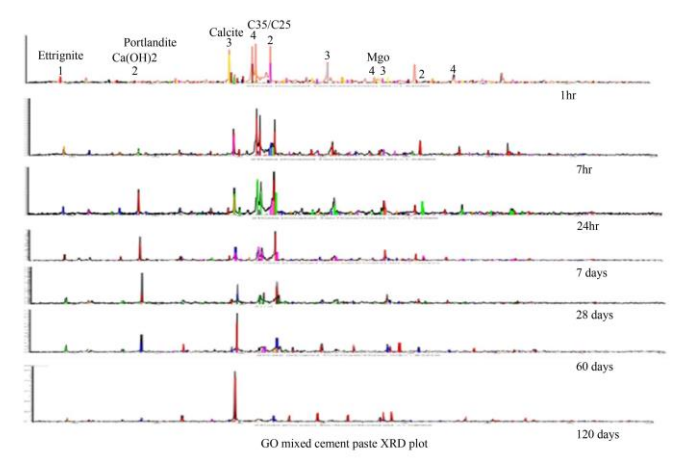


Fig. 10 XRD images of GO mixed cement paste - Transition phases

The calcium hydroxide peak diffraction patterns were seen at 18°, 28°, 34°, and 47°, similar to the observations by Wang et al. [25]. The peaks of (Ca (OH)₂) and calcite were reduced compared to earlier stages. The diffraction peak of SiO₂ disappeared at 28 days. Mowlaei et al. [48] also highlighted that GOs exhibit a slight reduction in peak intensities related to cement clinkers, such as C₂S, suggesting a more advanced level of cement hydration. This event is likely due to the superior dispersion of GOs, which boosts the overall hydration process and improves the structural development.

The peaks of calcium hydroxide have reduced compared to earlier stages, decreasing from 56% to 34%. The percentage of calcite increased to 75%, indicating the carbonation of calcium hydroxide as shown in Figure 11. The percentage of calcium silicate has reduced from 26% to 13%, meaning it has decreased by half, as shown in Figure 10 at 60 days. The peaks of calcium hydroxide further decreased from 34% to 9%, indicating the dissolution process and the formation of calcium silicate. The percentage of calcite increased to 88% from 75%, improving space filling and lowering porosity after 120 days. Other compounds, such as quartz, gypsum, and calcium aluminates, have decreased considerably due to the formation of cross-linking ions (Li et al., [49]), and the XRD peaks have flattened. This indicates the completion of the heat of hydration. A similar pattern for the crystal types of

hydration products was obtained by Suo et al. [50], which means that GO remains chemically inert to the hydration products, acting solely as a catalyst that enhances the structure and performance without altering the chemical dynamics.

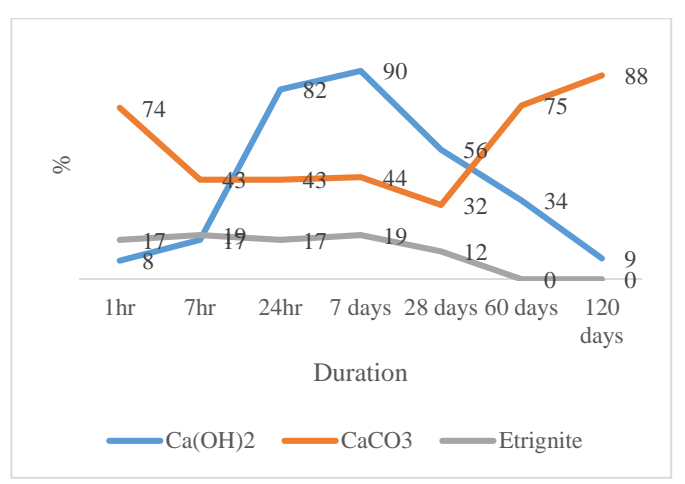


Fig. 11 Comparison of the duration (from 1 hour to 120 days) and the amount of Ca (OH)₂, CaCO₃, and ettringite in percentage from the XRD plots

4.5. EDAX Analysis of 0.03% GO Mixed Cement Paste - Transition Phases

A similar trend can be verified using the EDAX plot, as shown in Figure 12, 13, 14, and Figure 15. Calcium in hydroxide form breaks down over 7 days and forms a carbonated product. GO helps maintain oxygen levels. The Carbon (C) element represents 0.03% of the GO added, and the elemental Silicon (Si) was used for oxidation purposes. EDAX analysis, as revealed by Subramani and Ganesan [35], further demonstrates that the existence of silicon and calcium synergistically amplifies the cement composite's performance, driving its strength and stability to new heights. This suggests that GO increases the process of hydration, resulting in maximum strength gain within the first 7 days.

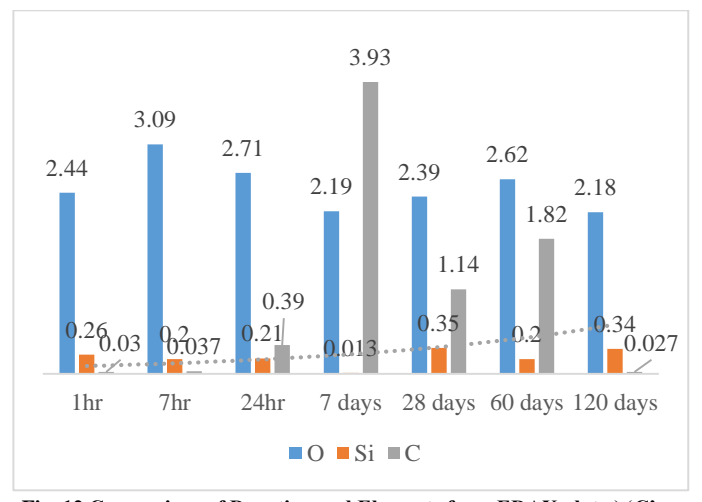


Fig. 12 Comparison of Duration and Elements from EDAX plot a) 'C', b) 'O', and c) 'Si'

4.6. Effect of GO on Crystal Size and Duration



Fig. 13 Effect of GO on crystal size and duration

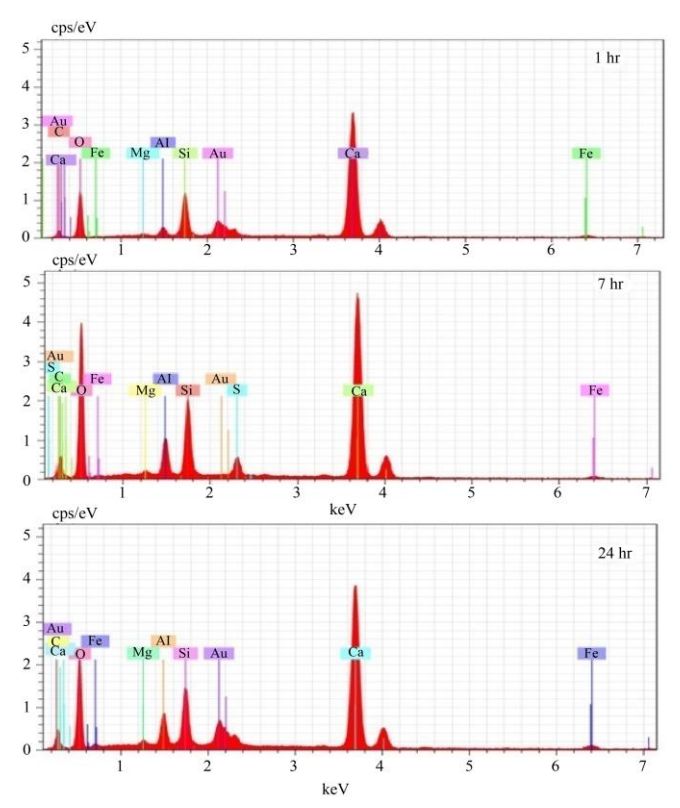


Fig. 14 EDAX images of GO mixed cement paste-Transition Phases 1hr,7hr and 24hr

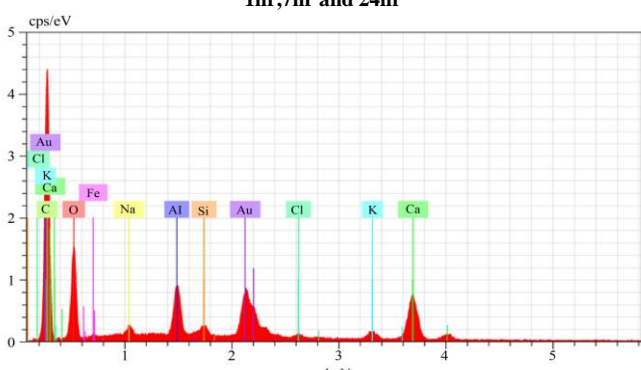
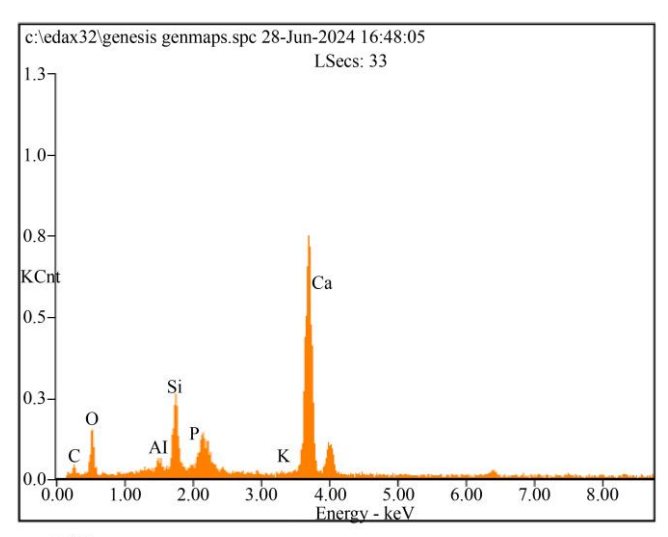


Fig. 15 EDAX images of GO mixed cement paste, Transition phases 7 days



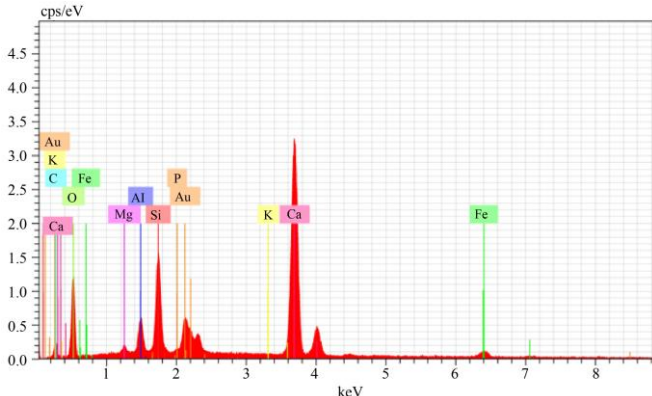


Fig. 16 EDAX images of GO mixed cement pastedays, 60days, 120 days

CH crystal sizes were calculated by the Debye Scherrer equation, [51]

$$D = (K \lambda) / (\beta \cos \theta)$$

Where is D = Grain dimensions orthogonal to the crystal level. The X-ray wavelength is denoted by λ , the diffraction angle is symbolized by θ , the diffraction peak half-width is indicated by β , K is an integer with a value of 0.89, and λ = 0.15406 nm. Crystal size is worked out from the full width at half maximum and peak position (θ) for a duration of 1 hour to 120 days. The CH size decreased from 92 nm to 82 nm within the first 7 hours, and then further decreased to 64 nm by 24 hours. From 24 hours to 7 days, it increased from 64 nm to 82 nm and remained the same until 120 days, as shown in Figure 16. Thus, it may be said that GO changes the size of CH's crystal, which stays constant between 7 and 120 days. This indicates the phenomenon of crystallization promotion in cement paste [52, 53].

4.7. Effect of GO on Ca/Si Ratio and Duration

Hajilar and Shaferi [54] used molecular simulation techniques to identify the elastic properties of hydrated cement pastes, along with analogous tobermorite, jennite, portlandite,

ettringite, and others. According to MD simulation results, the ideal Ca/Si ratio is between 1.3 and 2 for higher stiffness and tensile strength [55]. In C-S-H, a greater Ca/Si ratio results in structural flaws [56]. The Ca/Si ratio was calculated for 1 hour to 120 days, and the graph was plotted as shown in Figure 17. From the graph, the values were found close to 2, and the average value was found as 2.06, indicating that the GO's addition enhances the tensile strength and stiffness.

The lattice parameters of portlandite were (a) 3.59, (c) 4.90, Z (1), and volume 54.8, with the hexagonal nature of the crystals remaining constant for all durations mentioned above. A similar pattern was identified by Harutyunyan et al. [57]. On the other hand, the lattice parameters of ettringite were (a) 11.23, (c) 21.44, Z (2), and volume 2341.61, with the hexagonal nature of the crystals. This indicates an improvement in tensile strength, as found by Sindu et al. [58]. Considering the lattice characteristics and the Ca/Si ratio, the C-S-H structure was simulated using jennite and portlandite. Similar observations were made by Bonaccorsi et al. [59]. This suggests that no special compounds form, as identified by Dhamwardhana et al. [60].

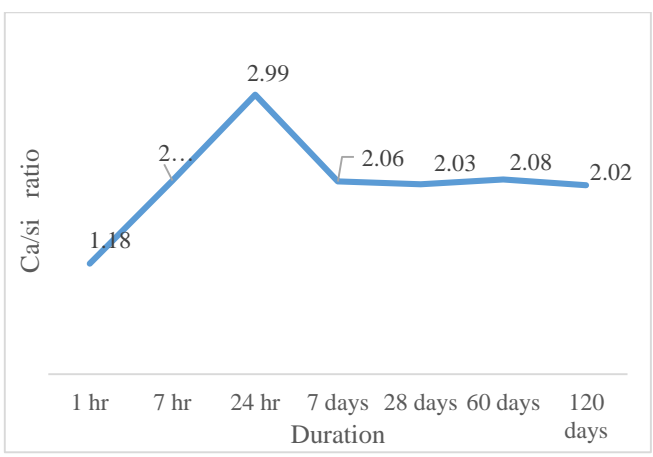


Fig. 17 Effect of GO on Ca/Si ratio and duration

According to Sindu et al. [49], the stiffness and cohesive forces of composites were reduced when Ca atoms were present in C-S-H. To get a higher tensile strength, the C-S-H lattice spacing between silicate chains should be a minimum.

5. Conclusion

3-day compressive strength demonstrates that GO boosts early strength development. The 7-day high strength could be the result of enhanced mechanical interlocking due to the addition of GO in concrete and significant interaction between tiny fissures and GO. Strength increases at 28 days as a result of an interface connection formed between carboxylic groups and hydration products, as GO speeds up the hydration process. Concrete's capacity to adjust to deformation is improved by GO. The high splitting tensile strength after 3 days and 7 days indicates the impact of GO's early strength accomplishment. Because of its vast surface area and ability

to form potent chemical bonds with cementitious materials like cement and concrete aggregates. Since GO is hundreds of times stronger than steel, it increases the splitting tensile strength of concrete after 28 days of mixing by strengthening the mixture as a tiny reinforcement. GO is crucial for the development of concrete's strength because it serves as an area of nucleation for C-S-H gels [61]. The hydration process is accelerated as a result. It facilitates the development of early flexural strength in 3 days. GO lessens stress concentration spots that can cause failure by distributing stress more evenly throughout the composite material after 7 days. Within 28 days, flexural strength increases because of GO's high intrinsic strength, homogenous stress distribution, and fracture bridging, and improved interfacial bonding.

The SEM images of GO-mixed cement paste after 1 hour show fibrous and granular calcium silicate structures with visible ettringite growth, while EDAX analysis suggests the presence of crystalline C-S-H (Jennite), which enhances the cement paste strength. After 7 hours, large agglomerated hydration clusters form, and needle-like ettringite crystals create an interconnected network that boosts compressive strength. EDAX analysis indicates that GO may either initiate or reinforce C-S-H formation. Within 24 hours, C-S-H formation increases, and GO creates a barrier effect, leading to the densification of hydration products and reduced porosity. The interaction between GO's functional groups and hydration components occurs after seven days, while the rodlike crystals eventually give way to flower-like formations on the GO surface. After 28 days, the hydration products become denser as rod-like crystals disappear and flower-like structures form, with GO improving the Interfacial Transition Zone (ITZ) and enhancing hydration kinetics for a more compact, less porous C-S-H gel. Within 60 days, a network forms within the pore structure, filling cracks, while flower-like and polyhedral crystals surround the needle structures, and AFM images show the surface. After 120 days, the surface becomes a dense, hardened paste with an icosahedral shape, and the transition of calcium carbonate occurs in three phases: from single cubic crystals to a second crystal phase.

XRD analysis shows that fullerite C60, present at 49% in early-stage liquid cement, represents GO in a closed mesh form, helping control the mixture's setting, while magnesite (32%) and eitelite (52%) are transient phases observed during magnesium formation after 1 hour. After 7 hours, large quantities of calcium silicate (82%) and calcite (43%) suggest incomplete hydration, indicating many cement clinkers remained unreacted. By 24 hours, hydration yields like calcium hydroxide (82%) and calcium silicate (84%) show a significant increase, demonstrating GO's role in enhancing the early heat of hydration and accelerating C₃S hydration. After 7 days, a 90% increase in (Ca (OH)₂) indicates a strong heat of hydration, with silica fumes converting it to calcium silicates, while GO continues to act as a nucleation site, resulting in stronger GO concrete compared to conventional

concrete in the early stages. It achieves 79% of the compressive strength, 93% of the split tensile strength, and 75% of the flexural strength in comparison to the 28-day strength. Overall, it reaches an average of 82% of the final 28day strength within 7 days, which is 26% higher than that of conventional concrete. At 28 days, reduced intensities for both (Ca (OH)₂) and calcite, indicating further hydration progression, likely due to the superior dispersion of GO. By 60 days, (Ca (OH)2) peaks decreased from 56% to 34%, while calcite increased to 75%, indicating carbonation of Ca (OH)2, and calcium silicate dropped from 26% to 13%. After 120 days, (Ca(OH)₂) decreased further, from 34% to 9%, while calcite reached 88%, enhancing space filling and reducing porosity. Other compounds, such as quartz, gypsum, and calcium aluminates, showed decreased XRD peaks, signaling the completion of hydration. EDAX analysis reveals that over seven days, 'Ca' in hydroxide form breaks down into a carbonated product, while GO helps maintain oxygen levels, with the 'C' element comprising 0.03% of the GO added. Additionally, elemental 'Si' was used for oxidation, suggesting that GO speeds up the process of hydration and helps to peak strength development during the crucial first 7 days.

The CH crystal size calculation shows that GO modifies the crystal structure, maintaining a consistent size from 7 to 120 days, highlighting its role in promoting crystallization within the cement paste. A higher Ca/Si ratio creates structural flaws in C-S-H. The average Ca/Si ratio of 2.06 and the uniform hexagonal nature of the ettringite crystals, based on the lattice parameter, suggest that GO enhances the tensile strength and stiffness of the cement paste without forming any special compounds.

5.1. Concluding Remarks

Finally, it can be concluded from mechanical strengths, SEM, and EDAX analyses that 0.03% GO enhances cement paste and concrete. Compressive strength was found to increase compared to regular concrete by 21%-32%. Concrete's flexural strength rises by 38%-48%, and its splitting tensile strength by 22%-35% when GO is added. It also helped to minimize fractures from forming and spreading, especially in areas where flexural stress is prevalent, owing to its high flexural strength to splitting tensile strength ratio of 1.72. It helps with cost reduction and thin-element design. As hydration progresses, the initial rod-like crystals disappear, giving way to flower-like and polyhedral structures, which become prominent by 60 days, with icosahedral shapes and cubic CaCO3 crystals forming by day 120. XRD analysis shows that fullerite C60, representing GO in a closed-mesh form, aids in early cement setting, while magnesite and eitelite appear as transient magnesium phases, which improve the density and refine pores. A 90% increase in Ca (OH)2 is observed at 7 days, which later converts to CaCO3 due to the action of silica fumes, indicating average early strength development by 82% and 26% higher than that of conventional concrete. EDAX confirms stable oxygen levels,

and the 0.03% GO concentration remains unchanged after 120 days, suggesting no unexpected compound formation. The CH crystal size increases from 64 nm to 82 nm by day 7 and then stabilizes, while portlandite and ettringite exhibit hexagonal structures with their respective lattice parameters, and the average Ca/Si ratio of 2.06 indicates improved mechanical performance due to GO addition. The incorporation of GO remarkably enhances the cement paste's morphology and elevates its mechanical strength, driving the development of high-performance, sustainable concrete for modern construction.

5.2. Future Challenges to Overcome

Despite the promising potential of GO-enhanced concrete, several challenges hinder its widespread adoption, including high cost, limited production scalability, and the difficulty of maintaining consistent quality and performance across batches.

The small-scale samples used in this study might not accurately reflect large-scale construction situations, where factors such as reinforcement, load distribution, and environmental conditions vary considerably. Moreover, concrete behavior can differ with geographic location, material sources, and climate—variables not entirely captured controlled laboratory conditions. In conclusion, while research and development on GOmodified concrete are still in progress, its future remains highly promising due to its potential to enhance strength, sustainability, and smart functionality. However, further innovation and extensive investigation are essential to enable its successful implementation in real-world construction applications.

Funding Statement

This study was carried out without the receipt of any funding.

References

- [1] Mugineysh Murali et al., "Utilizing Graphene Oxide in Cementitious Composites: A Systematic Review," *Case Studies in Construction Materials*, vol. 17, pp. 1-27, 2022. [CrossRef] [Google Scholar] [Publisher Link]
- [2] Shenghua Lv et al., "Effect of Graphene Oxide Nanosheets of Microstructure and Mechanical Properties of Cement Composites," *Construction and Building Materials*, vol. 49, pp. 121-127, 2013. [CrossRef] [Google Scholar] [Publisher Link]
- [3] Shenghua Lv et al., "Use of Graphene Oxide Nanosheets to Regulate the Microstructure of Hardened Cement Paste to Increase Its Strength and Toughness," *CrystEngComm*, vol. 16, no. 36, pp. 8508-8516, 2014. [CrossRef] [Google Scholar] [Publisher Link]
- [4] Shuaijie Lu et al., "Reinforcing Mechanisms Review of the Graphene Oxide on Cement Composites," *Nanotechnology Reviews*, vol. 13, no. 1, pp. 1-19, 2024. [CrossRef] [Google Scholar] [Publisher Link]
- [5] K.M. Lee, and J.H. Park, "A Numerical Model for Elastic Modulus of Concrete Considering Interfacial Transition Zone," *Cement and Concrete Research*, vol. 38, no. 3, pp. 396-402, 2008. [CrossRef] [Google Scholar] [Publisher Link]
- [6] M. Devasena, and J. Karthikeyan, "Investigation on Strength Properties of Graphene Oxide Concrete," *International Journal of Engineering Science Invention Research & Development*, vol. 1, pp. 307-310, 2015. [Google Scholar] [Publisher Link]
- [7] Valles Romero José Antonio, Cuaya-Simbro German, and Morales Maldonado Emilio Raymundo, "Optimizing Content Graphene Oxide in High Strength Concrete," *International Journal of Scientific Research and Management*, vol. 4, no. 6, pp. 4324-4332, 2016. [Google Scholar] [Publisher Link]
- [8] K.R. Mohammad Shareef, Shaik Abdul Rawoof, and K. Sowjanya, "A Feasibility Study on Mechanical Properties of Concrete with Graphene Oxide," *International Research Journal of Engineering and Technology*, vol. 4, no. 12, pp. 218-224, 2017. [Google Scholar] [Publisher Link]
- [9] Kandhunuri Srikanth, and T. Ashok, "An Experimental Study on Mechanical Properties of Concrete by Using Graphene Oxide," *International Journal of Research*, vol. 7, no. 10, pp. 150-154, 2018. [Publisher Link]
- [10] Jinwoo An et al., "Feasibility of using Graphene Oxide Nanoflake (GONF) as Additive of Cement Composite," *Applied Sciences*, vol. 8, no. 3, pp. 1-13, 2018. [CrossRef] [Google Scholar] [Publisher Link]
- [11] Zengshun Chen et al., "Modeling Shrinkage and Creep for Concrete with Graphene Oxide Nanosheets," *Materials*, vol. 12, no. 19, pp. 1-19, 2019. [CrossRef] [Google Scholar] [Publisher Link]
- [12] Sen Du et al., "Effect of Admixing Graphene Oxide on Abrasion Resistance of Ordinary Portland Cement Concrete," *AIP Advances*, vol. 9, no. 10, pp. 1-9, 2019. [CrossRef] [Google Scholar] [Publisher Link]
- [13] P.K. Akarsh et al., "Influence of Graphene Oxide on Properties of Concrete in the Presence of Silica Fumes and M-Sand," *Construction and Building Materials*, vol. 268, 2021. [CrossRef] [Google Scholar] [Publisher Link]
- [14] Sanglakpam Chiranjiakumari Devi, and Rizwan Ahmad Khan, "Effect of Sulfate Attack and Carbonation in Graphene Oxide–Reinforced Concrete Containing Recycled Concrete Aggregate," *Journal of Materials in Civil Engineering*, vol. 32, no. 11, 2020. [CrossRef] [Google Scholar] [Publisher Link]
- [15] Yihong Xu, and Yingfang Fan, "Effects of Graphene Oxide Dispersion on Salt-Freezing Resistance of Concrete," *Advances in Materials Science and Engineering*, vol. 2020, no. 1, pp. 1-9, 2020. [CrossRef] [Google Scholar] [Publisher Link]

- [16] Zengshun Chen et al., "Mechanical Properties and Shrinkage Behavior of Concrete-Containing Graphene-Oxide Nanosheets," *Materials*, vol. 13, no. 3, pp. 1-15, 2020. [CrossRef] [Google Scholar] [Publisher Link]
- [17] Namrata N. Chavan, and M.S. Karriappa, "An Experimental Investigation on Strength Properties of Concrete with Graphene Oxide," *International Research Journal of Engineering and Technology*, vol. 8, no. 1, pp. 1981-1984, 2021. [Publisher Link]
- [18] Osama Zaid et al., "Experimental Study on the Properties Improvement of Hybrid Graphene Oxide Fiber-Reinforced Composite Concrete," *Diamond and Related Materials*, vol. 124, pp. 1-12, 2022. [CrossRef] [Google Scholar] [Publisher Link]
- [19] Ali Jahami et al., "Effect of Graphene as Additive on the Mechanical Properties of Concrete," *NanoWorld Journal*, vol. 9, no. 2, pp. S87-S92, 2023. [Google Scholar] [Publisher Link]
- [20] Pooja Kaushik, Owais Ul Hassan, and Asif Hussain, "Impact of Graphene Insertion on the Workability of Concrete," *International Journal of Civil, Structural, Environmental and Infrastructure Engineering Research and Development*, vol. 14, no. 1, 2023. [Google Scholar]
- [21] Xiantong Yan et al., "Study of Optimizing Graphene Oxide Dispersion and Properties of the Resulting Cement Mortars," *Construction and Building Materials*, vol. 257, 2020. [CrossRef] [Google Scholar] [Publisher Link]
- [22] Wu-Jian Long et al., "Performance Enhancement and Environmental Impact of Cement Composites Containing Graphene Oxide with Recycled Fine Aggregates," *Journal of Cleaner Production*, vol. 194, pp. 193-202, 2018. [CrossRef] [Google Scholar] [Publisher Link]
- [23] Liulei Lu, and Dong Ouyang, "Properties of Cement Mortar and Ultra-High Strength Concrete Incorporating Graphene Oxide Nanosheets," *Nanomaterials*, vol. 7, no. 7, pp. 1-14, 2017. [CrossRef] [Google Scholar] [Publisher Link]
- [24] Danula Udumulla et al., "Effect of Graphene Oxide Nanomaterials on the Durability of Concrete: A Review on Mechanisms, Provisions, Challenges, and Future Prospects," *Materials*, vol. 17, no. 10, pp. 1-23, 2024. [CrossRef] [Google Scholar] [Publisher Link]
- [25] Liguo Wang et al., "Effect of Graphene Oxide (GO) on the Morphology and Microstructure of Cement Hydration Products," *Nanomaterials*, vol. 7, no. 12, pp. 1-10, 2017. [CrossRef] [Google Scholar] [Publisher Link]
- [26] Guo-jian Jing et al., "A Ball Milling Strategy to Disperse Graphene Oxide in Cement Composites," *New Carbon Materials*, vol. 34, no. 6, pp. 569-577, 2019. [CrossRef] [Google Scholar] [Publisher Link]
- [27] Tanvir S. Qureshi et al., "Nano-Cement Composite with Graphene Oxide Produced from Epigenetic Graphite Deposit," *Composites Part B: Engineering*, vol. 159, pp. 248-258, 2019. [CrossRef] [Google Scholar] [Publisher Link]
- [28] Donghoon Kang et al., "Experimental Study on Mechanical Strength of GO-Cement Composites," *Construction and Building Materials*, vol. 131, pp. 303-308, 2017. [CrossRef] [Google Scholar] [Publisher Link]
- [29] Li Zhao et al., "Mechanical Behavior and Toughening Mechanism of Polycarboxylate Superplasticizer Modified Graphene Oxide Reinforced Cement Composites," *Composites Part B: Engineering*, vol. 113, pp. 308-316, 2017. [CrossRef] [Google Scholar] [Publisher Link]
- [30] Lanzhen Yu, and Rongxing Wu, "Using Graphene Oxide to Improve the Properties of Ultra-High-Performance Concrete with Fine Recycled Aggregate," *Construction and Building Materials*, vol. 259, 2020. [CrossRef] [Google Scholar] [Publisher Link]
- [31] Shaoqiang Meng et al., "The Role of Graphene/Graphene Oxide in Cement Hydration," *Nanotechnology Reviews*, vol. 10, no. 1, pp. 768-778, 2021. [CrossRef] [Google Scholar] [Publisher Link]
- [32] Stefanos Mourdikoudis, Roger M. Pallares, and Nguyen T.K. Thanh, "Characterization Techniques for Nanoparticles: Comparison and Complementarity Upon Studying Nanoparticle Properties," *Nanoscale*, vol. 10, no. 27, pp. 12871-12934, 2018. [CrossRef] [Google Scholar] [Publisher Link]
- [33] Sanglakpam Chiranjiakumari Devi, and Rizwan Ahmad Khan, "Influence of Graphene Oxide on Sulfate Attack and Carbonation of Concrete Containing Recycled Concrete Aggregate," *Construction and Building Materials*, vol. 250, 2020. [CrossRef] [Google Scholar] [Publisher Link]
- [34] Hongyan Chu et al., "Effect of Graphene Oxide on Mechanical Properties and Durability of Ultra-High-Performance Concrete Prepared from Recycled Sand," *Nanomaterials*, vol. 10, no. 9, pp. 1-17, 2020. [CrossRef] [Google Scholar] [Publisher Link]
- [35] Kalaiselvi Subramani, and Arun Kumar Ganesan, "Synergistic Effect of Graphene Oxide and Coloidalnano-Silica on the Microstructure and Strength Properties of Fly Ash Blended Cement Composites," *Matéria (Rio de Janeiro)*, vol. 29, no. 1, pp. 1-17, 2024. [CrossRef] [Google Scholar] [Publisher Link]
- [36] Wengui Li et al., "A Comprehensive Review on Self-Sensing Graphene/Cementitious Composites: A Pathway toward Next-Generation Smart Concrete," *Construction and Building Materials*, vol. 331, 2022. [CrossRef] [Google Scholar] [Publisher Link]
- [37] Ali Al-Dahawi et al., "Electrical Percolation Threshold of Cementitious Composites Possessing Self-Sensing Functionality Incorporating Different Carbon-Based Materials," *Smart Materials and Structures*, vol. 25, no. 10, 2016. [CrossRef] [Google Scholar] [Publisher Link]
- [38] Changjiang Liu et al., "Studies on Mechanical Properties and Durability of Steel Fiber Reinforced Concrete Incorporating Graphene Oxide," *Cement and Concrete Composites*, vol.130, 2022. [CrossRef] [Google Scholar] [Publisher Link]
- [39] Miaomiao Hu et al., "Effect of Characteristics of Chemical Combined of Graphene Oxide-Nanosilica Nanocomposite Fillers on Properties of Cement-Based Materials," *Construction and Building Materials*, vol. 225, pp. 745-753, 2019. [CrossRef] [Google Scholar] [Publisher Link]

- [40] Huiting Liu et al., "Hybrid Effects of Nano-Silica and Graphene Oxide on Mechanical Properties and Hydration Products of Oil Well Cement," Construction and Building Materials, vol. 191, pp. 311-319, 2018. [CrossRef] [Google Scholar] [Publisher Link]
- [41] Karthik Chintalapudi, and Rama Mohan Rao Pannem, "The Effects of Graphene Oxide Addition on Hydration Process, Crystal Shapes, and Microstructural Transformation of Ordinary Portland Cement," *Journal of Building Engineering*, vol. 32, 2020. [CrossRef] [Google Scholar] [Publisher Link]
- [42] Ramanjit Kaur, and N.C. Kothiyal, "Positive Synergistic Effect of Superplasticizer Stabilized Graphene Oxide and Functionalized Carbon Nanotubes as a 3-D Hybrid Reinforcing Phase on the Mechanical Properties and Pore Structure Refinement of Cement Nanocomposites," *Construction and Building Materials*, vol. 222, pp. 358-370, 2019. [CrossRef] [Google Scholar] [Publisher Link]
- [43] Gen Li, and L.W. Zhang, "Microstructure and Phase Transformation of Graphene-Cement Composites Under High Temperature," *Composites Part B: Engineering*, vol. 166, pp. 86-94, 2019. [CrossRef] [Google Scholar] [Publisher Link]
- [44] Tanvir S. Qureshi, and Daman K. Panesar, "Impact of Graphene Oxide and Highly Reduced Graphene Oxide on Cement Based Composites," *Construction and Building Materials*, vol. 206, pp. 71-83, 2019. [CrossRef] [Google Scholar] [Publisher Link]
- [45] P.K. Akarsh et al., "Influence of Graphene Oxide on Properties of Concrete in the Presence of Silica Fumes and M-Sand," *Construction and Building Materials*, vol. 268, 2021. [CrossRef] [Google Scholar] [Publisher Link]
- [46] Hongzhi Cui et al., "Possible Pitfall in Sample Preparation for SEM Analysis A Discussion of the Paper "Fabrication of Polycarboxylate/Graphene Oxide Nanosheet Composites by Copolymerization for Reinforcing and Toughening Cement Composites," by Lv et al.," *Cement and Concrete Composites*, vol. 77, pp. 81-85, 2017. [CrossRef] [Google Scholar] [Publisher Link]
- [47] Jinwoo An et al., "Edge-Oxidized Graphene Oxide (EOGO) in Cement Composites: Cement Hydration and Microstructure," *Composites Part B: Engineering*, vol. 173, 2019. [CrossRef] [Google Scholar] [Publisher Link]
- [48] Roozbeh Mowlaei et al., "The Effects of Graphene Oxide-Silica Nanohybrids on the Workability, Hydration, and Mechanical Properties of Portland Cement Paste," *Construction and Building Materials*, vol. 266, 2021. [CrossRef] [Google Scholar] [Publisher Link]
- [49] Xiangyu Li et al., "Effects of Graphene Oxide Agglomerates on Workability, Hydration, Microstructure and Compressive Strength of Cement Paste," *Construction and Building Materials*, vol. 145, pp. 402-410, 2017. [CrossRef] [Google Scholar] [Publisher Link]
- [50] Yuxia Suo et al., "Study on Modification Mechanism of Workability and Mechanical Properties for Graphene Oxide-Reinforced Cement Composite," *Nanomaterials and Nanotechnology*, vol. 10, pp. 1-12, 2020. [CrossRef] [Google Scholar] [Publisher Link]
- [51] A.L. Patterson, "The Scherrer Formula for X-Ray Particle Size Determination," *Physical Review*, vol. 56, no. 10, 1939. [CrossRef] [Google Scholar] [Publisher Link]
- [52] Jeffrey J. Chen et al., "A Coupled Nanoindentation/SEM-EDS Study on Low Water/Cement Ratio Portland Cement Paste: Evidence for C–S–H/Ca(OH)₂ Nanocomposites," *Journal of the American Ceramic Society*, vol. 93, no. 5, pp.1484-1493, 2010. [CrossRef] [Google Scholar] [Publisher Link]
- [53] Kai Gong et al., "Reinforcing Effects of Graphene Oxide on Portland Cement Paste," *Journal of Materials in Civil Engineering*, vol. 27, no. 2, 2015. [CrossRef] [Google Scholar] [Publisher Link]
- [54] Shahin Hajilar, and Behrouz Shafei, "Nano-Scale Investigation of Elastic Properties of Hydrated Cement Paste Constituents Using Molecular Dynamics Simulations," Computational Materials Science, vol. 101, pp. 216-226, 2015. [CrossRef] [Google Scholar] [Publisher Link]
- [55] Dongshuai Hou et al., "Nano-Scale Mechanical Properties Investigation of CSH from Hydrated Tri-Calcium Silicate by Nano-Indentation and Molecular Dynamics Simulation," *Construction and Building Materials*, vol. 189, pp. 265-275, 2018. [CrossRef] [Google Scholar] [Publisher Link]
- [56] Davoud Tavakoli et al., "Multi-Scale Approach from Atomistic to Macro for Simulation of the Elastic Properties of Cement Paste," *Iranian Journal of Science and Technology, Transactions of Civil Engineering*, vol. 44, no. 3, pp. 861-873, 2020. [CrossRef] [Google Scholar] [Publisher Link]
- [57] V.S. Harutyunyan et al., "Investigation of Early Growth of Calcium Hydroxide Crystals in Cement Solution by Soft X-Ray Transmission Microscopy," *Journal of Materials Science*, vol. 44, no. 4, pp. 962-969, 2009. [CrossRef] [Google Scholar] [Publisher Link]
- [58] B.S. Sindu, Aleena Alex, and Saptarshi Sasmal, "Studies on Structural Interaction and Performance of Cement Composite Using Molecular Dynamics," *Advances in Computational Design*, vol. 3, pp. 147-163, 2018. [CrossRef] [Google Scholar] [Publisher Link]
- [59] Elena Bonaccorsi, Stefano Merlino, and H.F.W. Taylor, "The Crystal Structure of Jennite, Ca₉Si₆O₁₈(OH)₆·8H₂O," *Cement and Concrete Research*, vol. 34, no. 9, pp. 1481-1488, 2004. [CrossRef] [Google Scholar] [Publisher Link]
- [60] C.C. Dharmawardhana, A. Misra, and Wai-Yim Ching, "Quantum Mechanical Metric for Internal Cohesion in Cement Crystals," *Scientific Reports*, vol. 4, no. 1, pp. 1-8, 2014. [CrossRef] [Google Scholar] [Publisher Link]
- [61] Ali Bagheri et al., "Graphene Oxide-Incorporated Cementitious Composites: A Thorough Investigation," *Materials Advances*, vol. 3, no. 24, pp. 9040-9051, 2022. [CrossRef] [Google Scholar] [Publisher Link]

Appendix 1 Abbreviations

Sr. No.	Abbreviation	Description
1	Ca	Calcium
2	Ca (OH) ₂	Calcium hydroxide
3	CaCO ₃	Calcite, calcium carbonate
4	C-S-H	Calcium silicate hydrates
5	CTM	Compression testing machine
6	EDAX	Energy dispersive X-ray analysis
7	FESEM	Field emission scanning electron microscopy
8	GO	Graphene oxide
9	IS	Indian standard
10	ITZ	Interfacial transition zone
11	OPC	Ordinary Portland cement
12	SEM	Scanning electron microscopy
13	Si	Slica
14	SiO ₂	Silicon dioxide
15	UNFCCC	United Nations Framework Convention on Climate Change
16	wt.	Weight
17	XRD	X-ray diffraction